



A Convenient Method to Prepare C-F Codoped TiO₂ Catalyst

S.Z. HU^{1*}, L. MA², F.Y. LI¹ and Z.P. FAN¹

¹Institute of Eco-environmental Sciences, Liaoning Shihua University, Fushun 113001, P.R. China

²School of Petrochemical Engineering, Liaoning Shihua University, Fushun 113001, P.R. China

*Corresponding author: Tel: +86 24 23847473; E-mail: hushaozheng001@163.com

Received: 15 July 2013;

Accepted: 21 August 2013;

Published online: 10 May 2014;

AJC-15150

The C-F codoped TiO₂ catalysts were prepared by a simple CF₄ plasma treatment. X-ray diffraction, UV-visible spectroscopy, photoluminescence and X-ray photoelectron spectroscopy were used to characterize the prepared TiO₂ samples. The visible light absorption was obviously improved by C-F codoping. The doping amounts of F and C increased with increasing the discharge time. High discharge voltage led to the more favourable formation of the doping carbon and fluorine, whereas low discharge voltage led to the formation of surface fluorine and carbon film, caused the low doping amount. The photocatalytic activities of prepared TiO₂ catalysts were tested in the degradation of 2,4,6-trichlorophenol under both UV and visible light. The possible mechanism was proposed.

Keywords: TiO₂, C-F codoping, Plasma, CF₄, Visible light.

INTRODUCTION

Although various oxide semiconductors have been found possess the photocatalytic ability, TiO₂ is still the most important photocatalyst due to its biological and chemical inertness, strong oxidizing power, non-toxicity and long-term stability against photo-corrosion. However, a major barrier to the widespread use of TiO₂ as photocatalysts is its relatively large electronic band gap, some 3.0-3.2 eV, limiting its photo-response to visible light, which comprised of about 43 % of the incoming solar energy. In order to extend the photoresponse of TiO₂ into the visible region of the solar spectrum, considerable efforts have been directed towards the doping of TiO₂ lattice to modify its electronic band gap and shift its absorption edge to the visible light region.

One way to achieve this modification is to dope TiO₂ with non-metal. Recently, the possibility of two nonmetal dopants co-doping simultaneously has received much more attention. Several researchers have demonstrated the photocatalytic activity of nonmetal co-doping of TiO₂. Yang *et al.*¹ prepared fluorine, sulfur co-doped TiO₂ using solvothermal method. They believed that the co-doping gives rise to a localized state in the band gap of the oxide and creates active surface oxygen vacancies, both which are responsible for visible light absorption and the promotion of electrons from the localized states to the conduction band, thus increase the visible light activity of methylene blue degradation. Dolat *et al.*² prepared nitrogen, carbon co-doped TiO₂ by one-step hydrothermal method. They

found that the nature of the alcohol used as carbon precursor have a significant role on the optical (absorption of radiation) and physico-chemical (surface area, particle and crystallite size) properties of the modified materials. Wu *et al.*³ prepared carbon, boron co-doped TiO₂ material by gel-hydrothermal method. They suggested that coke carbon generated on the carbon doped TiO₂ surface act as a photosensitizer and has the photosensitization effect under the visible light.

Non-thermal plasma is composed of atoms, ions and electrons, which are much more reactive than their molecule precursors. Plasma is able to initiate a lot of reactions, which take place efficiently only at elevated temperatures and high pressures, under mild conditions, thus is used frequently to prepare functional nanomaterials. Here, we reported a convenient method to prepare C-F codoped TiO₂ catalyst by CF₄ plasma treatment. 2,4,6-Trichlorophenol was used as model molecules to investigate the photoactivity of obtained TiO₂ catalysts. The possible mechanism was proposed.

EXPERIMENTAL

P25 was annealed at 400 °C for 2 h to get rid of the adsorbed substance. The F and C doping was conducted in a dielectric barrier discharge (DBD) reactor, consisting of a quartz tube and two electrodes. The high-voltage electrode was a stainless-steel rod (2.5 mm), which was installed in the axis of the quartz tube and connected to a high voltage supply. The grounding electrode was an aluminum foil which was wrapped around the quartz tube. For each run, 0.4 g P25 was

charged into the quartz tube. At a constant CF_4 flow (30 mL min^{-1}), a high voltage of 12 kV was supplied by a plasma generator at an overall power input of $70 \text{ V} \times 0.5 \text{ A}$. The discharge frequency was fixed at 10 kHz and the discharge was kept for 20 min. After discharge, the reactor was cooled down to room temperature. The obtained material was denoted as M-70, where 70 stands for the discharge voltage. When the power input were $50 \text{ V} \times 0.5 \text{ A}$, $60 \text{ V} \times 0.5 \text{ A}$ and $80 \text{ V} \times 0.5 \text{ A}$ following the same procedure as in the synthesis of M-70, the obtained materials were denoted as M-50, M-60 and M-80.

XRD patterns of the prepared TiO_2 samples were recorded on a Rigaku D/max-2400 instrument using $\text{CuK}\alpha$ radiation ($\lambda = 1.54 \text{ \AA}$). UV-Visible spectroscopy measurement was carried out on a Jasco V-550 spectrophotometer, using BaSO_4 as the reference sample. Photoluminescence spectra were measured at room temperature with a fluorospectrophotometer (FP-6300) using an Xe lamp as excitation source. XPS measurements were conducted on a Thermo Escalab 250 XPS system with $\text{AlK}\alpha$ radiation as the exciting source. The binding energies were calibrated by referencing the C 1s peak (284.6 eV) to reduce the sample charge effect.

Suspensions were prepared in deionized water by mixing TiO_2 catalyst with appropriate solutions of 2,4,6-trichlorophenol. In a typical procedure, 0.1 g TiO_2 powders were dispersed in 100 mL solution of 2,4,6-trichlorophenol (initial concentration $C_0 = 60 \times 10^{-6} \text{ g mL}^{-1}$) in an ultrasound generator for 10 min. The suspension was transferred into a self-designed glass reactor and stirred for 0.5 h in darkness to achieve the adsorption equilibrium. In the photoreaction under visible light irradiation, the suspension was exposed to a 110 W high-pressure sodium lamp with main emission in the range of 400–800 nm and air was bubbled at 130 mL/min through the solution. The UV light portion of sodium lamp was filtered by 0.5 M NaNO_2 solution. All runs were conducted at ambient pressure and $30 \text{ }^\circ\text{C}$. The conversion of 2,4,6-trichlorophenol was determined using an Agilent 1100 series HPLC operated in isocratic mode under the following conditions: methanol-water (80:20 %); flow rate 1 mL min^{-1} ; temperature $25 \text{ }^\circ\text{C}$; Column Phenomenex Luna 10μ Phenyl-Hexyl, $4.6 \text{ mm} \times 250 \text{ mm}$; detector UV at 254 nm; injection volume $5 \mu\text{L}$.

RESULTS AND DISCUSSION

The XRD patterns of P25 and prepared plasma treated catalysts (not shown here) indicate that all TiO_2 samples were mixture of anatase phase and rutile phase. The phase component and the particle sizes of P25 and prepared catalysts were calculated by their XRD patterns according to the method of Spurr and Debye-Scherrer equation respectively^{4,5}. The results (not shown here) indicated that there is no obvious change in phase component and particle sizes among prepared catalysts.

Fig. 1 shows the UV-visible spectra of P25 and plasma treated catalysts. Compared with the spectra of P25, distinct shifts of the absorption bands into the visible light region were observed for plasma treated catalysts, which should result from the doping effect, leading to a narrowed band gap energy. The band gaps of the TiO_2 samples were calculated according the method of O'Regan and Gratzel⁶. The result indicates that the band gaps of plasma treated samples were 2.7 eV, which is

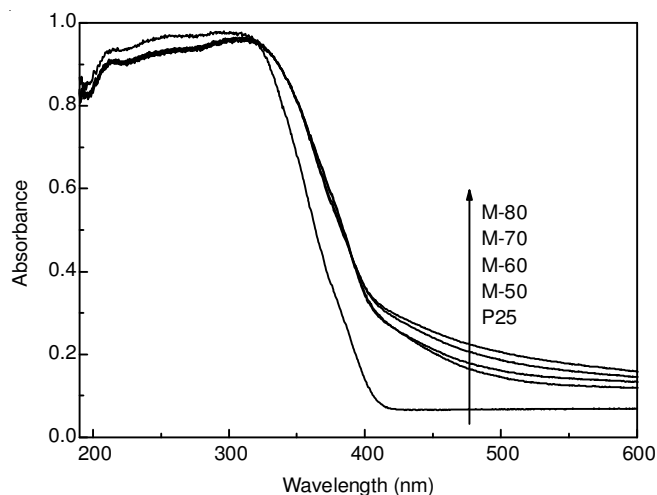


Fig. 1. UV-visible spectra of P25 and plasma treated catalysts

obviously lower than that of P25 (3.1 eV). It is of great importance for its practical application since it could be activated even by sunlight. Besides, a broad absorption in visible light region ($> 400 \text{ nm}$) is observed for all the plasma treated samples, accompanied with the changes of colour from white to gray. According to report of Ozaki *et al.*⁷, such broad absorption is attributed to the presence of Ti^{3+} and oxygen vacancies. It is reported that fluorine ions doped into TiO_2 lattice lead to favourable formation of Ti^{3+} and oxygen vacancies because of the charge compensation between^{8,9} F^- and Ti^{4+} . Therefore, such Ti^{3+} and oxygen vacancies were attributed to the F doping formed by the plasma treatment.

Compared with the spectra of P25, obvious shifts to lower binding energies were observed for CF_4 plasma treated catalysts in Ti 2p region (Fig. 2a). It is known that the binding energy of the element is influenced by its electron density. An increase of binding energy implies the lowering of the electron density. Therefore, such lower binding energies are due to the presence of Ti ion with low valence (Ti^{3+}), which exhibit the higher electron density. Those Ti^{3+} ions was probably attributed to the F doped into TiO_2 lattice which caused the charges imbalance. This is consistent with the UV-visible result. Similar results were reported by many researchers. Yu *et al.*¹⁰ explained the formation of Ti^{3+} ions through the charge compensation between F^- and Ti^{4+} . Li *et al.*¹¹ also found the Ti^{3+} ions were formed in F doped TiO_2 by ESR. In F 1s region (Fig. 2b), two peaks which located at 684.4 and 689.6 eV were observed. According to the previous reports, the peak located at 684.4 eV was attributed to the surface fluoride formed by ligand exchange between F^- and surface hydroxyl group on TiO_2 ¹². The higher binding energy around 689.4 eV could be ascribed to the F atom doped into TiO_2 lattice by substituting for an O atom^{13,14}.

The peaks in the C 1s region (Fig. 2c) were deconvoluted into three contributions. The peak around 284.6 eV was attributed to the C-C group, which probably formed by the plasma treatment. The peak at 288.6 eV was attributed to the carbon doped into TiO_2 lattice to form Ti-O-C structure. Another peak at higher binding energy 291.5 eV was probably attributed to the electron-deficiency of the C atom in the C-F bond. The amounts of F and C in different state determined

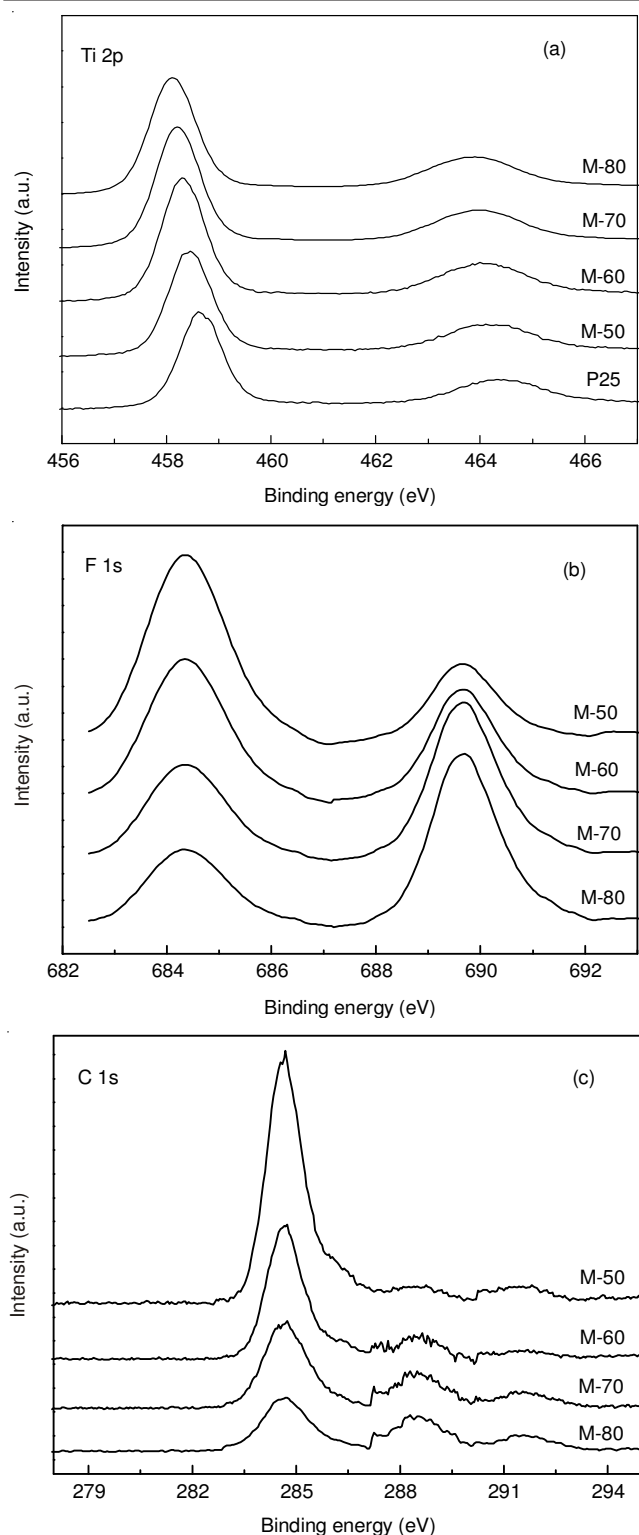


Fig. 2. XPS spectra of P25 and plasma treated catalysts in the region of Ti 2p (a), F 1s (b) and C 1s (c)

by XPS spectra are summarized in Table-1. Obviously, the amounts of doping F and C increased with increasing the discharge voltage from 50 to 80 V, whereas the surface F and C amounts exhibited the contrary trend, decreased with increasing the discharge voltage. This indicated that high discharge voltage lead to the more favourable formation of the doping fluorine and carbon, whereas low discharge voltage led to the formation of surface fluorine and carbon film.

TABLE-1
AMOUNTS OF F AND C IN DIFFERENT STATE IN THE PLASMA TREATED TiO₂ CATALYSTS

Catalysts	Doping F amount (at.%)	Surface F amount (at.%)	Doping C amount (at.%)	Adsorbed C amount (at.%)
M-50	0.6	1.9	0.2	2.6
M-60	1.0	1.5	0.4	1.6
M-70	1.9	1.0	0.6	1.1
M-80	2.1	0.8	0.6	0.8

Tables 2 and 3 exhibit the amounts of F and C in different state in the catalysts prepared under 70 and 50 V discharge voltage. Obviously, the doping F amount is higher than doping C amount under 70 V discharge voltage. With the increase of discharge time, the amounts of F and C in different state (doping F, doping C, surface F and adsorbed C) increased. Under 50 V discharge voltage, the doping F and C amounts were obvious lower than that prepared under 70 V discharge voltage with the same discharge time, whereas the surface F and adsorbed C amounts were obvious higher than that prepared under 70 V discharge voltage. Besides, the doping F and C amounts increased slightly with increasing the discharge time under 50 V discharge voltage. This is probably due to that most of F and C atoms covered the TiO₂ surface to form fluorine and carbon films, which inhibited the doping of C and F with increasing the discharge time. These results confirmed the conclusion that high discharge voltage led to the more favourable formation of the doping carbon and fluorine, whereas low discharge voltage led to the formation of surface fluorine and carbon film, caused the low doping amount.

TABLE-2
AMOUNTS OF F AND C IN DIFFERENT STATE IN THE CATALYSTS PREPARED UNDER 70 V DISCHARGE VOLTAGE

Discharge time (min)	Doping F amount (at.%)	Surface F amount (at.%)	Doping C amount (at.%)	Adsorbed C amount (at.%)
5	0.6	0.3	0.2	0.5
10	1.1	0.6	0.3	0.8
20	1.9	1.0	0.6	1.5
30	2.7	1.4	0.8	1.9

TABLE-3
AMOUNTS OF F AND C IN DIFFERENT STATE IN THE CATALYSTS PREPARED UNDER 50 V DISCHARGE VOLTAGE

Discharge time (min)	Doping F amount (at.%)	Surface F amount (at.%)	Doping C amount (at.%)	Adsorbed C amount (at.%)
5	0.4	0.6	0	1.4
10	0.5	1.0	0.1	2.0
20	0.6	1.9	0.2	2.6
30	0.6	2.0	0.2	3.7

Figs. 3 and 4 show the photocatalytic performances of P25 and plasma treated catalysts in the degradation of 2,4,6-trichlorophenol under visible and UV light irradiation. Under visible light (Fig. 3), P25 shows poor photocatalytic activity, whereas plasma treated TiO₂ catalysts exhibit obviously improved activities in the degradation of 2,4,6-trichlorophenol. This is due to the co-doping effect of C and F which much narrowed the band gap energy, leading to the visible light

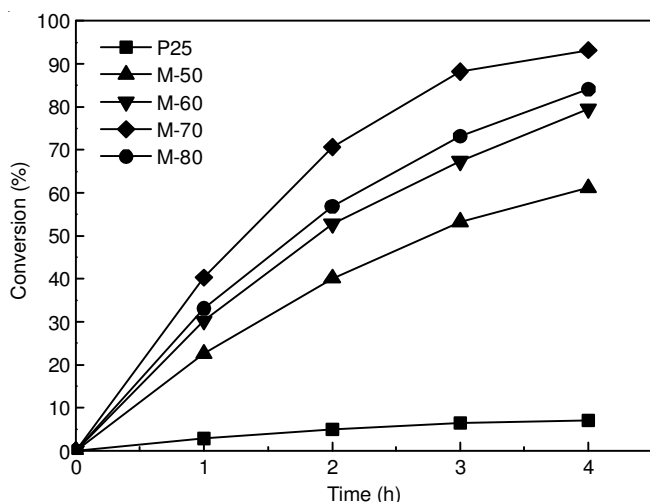


Fig. 3. Photocatalytic performances of P25 and plasma treated catalysts in the degradation of 2,4,6-trichlorophenol under visible light irradiation

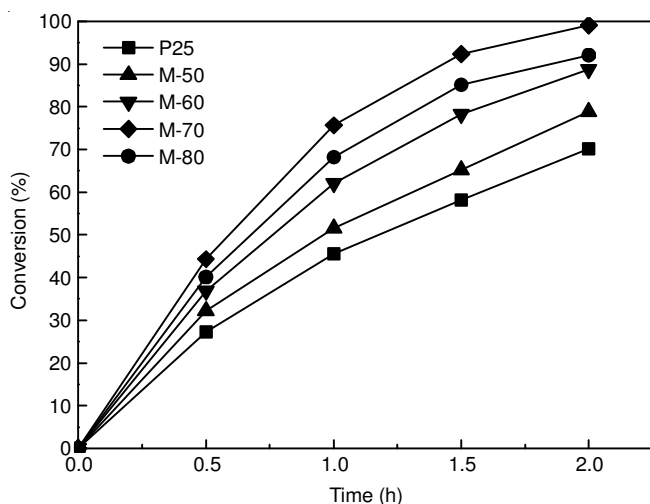


Fig. 4. Photocatalytic performances of P25 and plasma treated catalysts in the degradation of 2,4,6-trichlorophenol under UV light irradiation

absorption obviously increased. The degradation activity increased with increasing the discharge voltage firstly and then decreased when the discharge voltage beyond 70 V. This is due to the doping amounts were higher than the optimal value under 80 V discharge voltage, the doping site became the recombination center of electron-hole, leading to the decrease of separation efficiency. Under UV light (Fig. 4), the plasma treated TiO₂ catalysts also exhibit higher photocatalytic activities than that of P25. Moreover, the activities follow the order: P25 < M-50 < M-60 < M-80 < M-70, which is consistent with the contrary order of photoluminescence intensity. This indicated that the increase in the electron-hole separation rate caused by C-F codoping led to the increased degradation activities of plasma treated TiO₂ catalysts under UV light. Besides, the increased surface acidity caused by F doping led to the adsorption capacity of 2,4,6-trichlorophenol on TiO₂ surface remarkably

increased, which plays a significant important role in the increased degradation activities of plasma treated TiO₂ catalysts under both UV and visible light.

Conclusion

The C-F codoped TiO₂ catalyst was prepared by a simple CF₄ plasma treatment. The visible light absorption was obviously improved by C-F codoping. High discharge voltage led to the more favourable formation of the doping carbon and fluorine, whereas low discharge voltage led to the formation of surface fluorine and carbon film, caused the low doping amount. Under high discharge voltage, the amounts of F and C in different state increased with increasing the discharge time. However, under low discharge voltage, most of F and C atoms covered the TiO₂ surface to form fluorine and carbon films, which inhibited the doping of C and F with increasing the discharge time. The photocatalytic activities of plasma treated TiO₂ catalysts in the degradation of 2,4,6-trichlorophenol were obviously improved compared with P25 under both UV and visible light. This is due to the co-doping effect of C and F which much narrowed the band gap energy, leading to the visible light absorption obviously increased.

ACKNOWLEDGEMENTS

This work was supported by Program for New Century Excellent Talents in University (No. NCET-11-1011), National Natural Science Foundation of China (No. 41071317, 30972418, 21103077), National Key Technology R & D Programme of China (No. 2007BAC16B07, 2012ZX07505-001), the Natural Science Foundation of Liaoning Province (No. 20092080).

REFERENCES

- G.D. Yang, Z. Jiang, H.H. Shi, M.O. Jones, T.C. Xiao, P.P. Edwards and Z.F. Yan, *Appl. Catal. B*, **96**, 458 (2010).
- D. Dolat, N. Quici, E. Kusiak-Nejman, A.W. Morawski and G. Li Puma, *Appl. Catal. B*, **115-116**, 81 (2012).
- Y.M. Wu, M.Y. Xing and J.L. Zhang, *J. Hazard. Mater.*, **192**, 368 (2011).
- R.A. Spurr and H. Myers, *Anal. Chem.*, **29**, 760 (1957).
- J. Lin, Y. Lin, P. Liu, M.J. Meziani, L.F. Allard and Y.P. Sun, *J. Am. Chem. Soc.*, **124**, 11514 (2002).
- B. O'Regan and M. Gratzel, *Nature*, **353**, 737 (1991).
- H. Ozaki, N. Fujimoto, S. Iwamoto and M. Inoue, *Appl. Catal. B*, **70**, 431 (2007).
- D. Li, N. Ohashi, S. Hishita, T. Kolodiazny and H. Haneda, *J. Solid State Chem.*, **178**, 3293 (2005).
- A.E. Giannakas, E. Seristatidou, Y. Deligiannakis and I. Konstantinou, *Appl. Catal. B*, **132-133**, 460 (2013).
- J.C. Yu, J. Yu, W. Ho, Z. Jiang and L. Zhang, *Chem. Mater.*, **14**, 3808 (2002).
- D. Li, N. Ohashi, S. Hishita, T. Kolodiazny and H. Haneda, *J. Solid State Chem.*, **178**, 3293 (2005).
- W. Wang, C.H. Lu, Y.R. Ni, M.X. Su and Z.Z. Xu, *Appl. Catal. B*, **127**, 28 (2012).
- Y. Huo, Y. Jin, J. Zhu and H. Li, *Appl. Catal. B*, **89**, 543 (2009).
- X. Chen, Y. Su, X. Zhang and L. Lei, *Chin. Sci. Bull.*, **53**, 1983 (2008).